Bulg. J. Phys. **32** (2005) 292–301

Complex Phase Shift Interpretation for Distorted Wave of Elastic Pion Scattering from Nuclei

R. Safari

Department of Nuclear Physics, Faculty of Physics, Tabriz University, Tabriz , Iran

Received *October 20, 2005*

Abstract. We use the equivalent local form of Kisslinger optical potential to calculate the elastic differential cross-sections for the scattering of pions from $^{208}_{82}$Pb and $^{12}_{6}$C nuclei in the energy range of 150 to 292 MeV. For this range of energy the scattering amplitude depends on complex phase shifts of pion-nucleon interaction arising from spin and isospin degrees of freedom. We calculate the elastic differential cross-section by using Born approximation method. To get the desired results it is necessary to use a distorted wave function for the incident pions instead of the usual plane waves. This wave function has adjustable energy dependent parameters. By comparison of the experimental and theoretical differential cross-section, we have calculated the values of both potential and wave function parameters. We have used different density distributions to check their effects on angular distribution.

PACS number: 25.80.Dj, 25.80.-e

1 Introduction

The pion-nucleus elastic scattering below and above the (3,3) resonance has been extensively studied since the beginning of the 70's and significant experimental and theoretical investigations have been carried out till now. Experimental data with incident pion energies below the 300 MeV, *i.e.* below the range of the first pion- nucleon resonance, Δ_{33} , belong to 70's and the beginning of 80's, but a variety of theoretical models have been proposed to describe this very important physical interaction. References [1–5] present some of the recent theoretical model calculations about this subject.

In this paper we have used the Kisslinger optical potential (KOP) which was calculated by microscopic impulse approximation method [6]. This potential has two local and non-local terms and becomes important when the s and p

incident waves are in resonance. Johnson and Satchler [7] derived a local potential equivalent to non-local Kisslinger type potential on the basis of multiple scattering theory.We have used this potential to calculate the differential cross-sections for charged pions elastic scattering from different nuclei at low energies using the Born approximation (BA) [8]. We think that pion-nucleon two-body interaction becomes stronger at intermediate energies for larger distances from the center of the nucleus, which causes pions not to penetrate deeper in the nucleus. Therefore, the elastic scattering cross-section would have a considerable increase, which is not consistent with the values obtained from KOP with BA. In fact, having related the scattering amplitude to the spin and isospin degrees of freedom would cause to increase the strength of the potential at intermediate energies. Producing such a relation the scattering amplitude is related to the complex phase shifts by means of the attenuation coefficient η_l of the l^{th} partial wave, where η_l takes values between 0 and 1. Therefore, the scattering amplitude, which contains spin and isospin degrees of freedom becomes as a function of inelasticity coefficient ξ_l of partial wave scattering amplitude. To include the effect of these considerations in our basic calculation, we suppose that the wave number of the incident plane wave is altered and the scattering amplitude, $f(\theta_{sc})$, is the amplitude of the waves centered on the target nucleus with an effective wave number. The amplitude of this wave is related to energy. It is chosen as a function of distance and scattering angle. This consideration without theoretical calculation has been applied to compare the angular distribution of $^{208}_{82}$Pb interaction with data [9]. The complete theoretical arguments are presented here and the differential cross-section for the elastic scattering of negative pion from a light carbon and a heavy Pb targets using different density distributions at different energies are compared with data. Therefore, an initial distorted wave function ψ_i^d is introduced at the nuclear surface. In Section 2 we briefly explain the local form of the KOP. Our attempt to outline the above mentioned idea is considered in Section 3. We suppose that the pion-nucleus scattering depends on density distributions of nucleons of a nucleus. The discussion related to this matter is explained in Section 4. Finally Section 5 presents the comparison of our theoretical results of elastic scattering cross-sections for $^{208}_{82}$Pb and $^{12}_{6}$C nuclei with those of experimental data. Our discussions and conclusions are also considered in this section.

2 Local Potential Formalism

The actual KOP form for the scattering of pions from a nucleus in an appropriate units is written as follows:

$$U_k(r) = \frac{(\hbar c)^2}{2\omega}.(q(r) + \nabla.\alpha(r)\nabla). \tag{1}$$

The local transformed form of this potential is calculated from a Shrodinger-like equation, which is obtained from a Klein Gordan equation by using the Krell-

Ericson transformation [10]

$$U_L = \frac{(\hbar c)^2}{2\omega}\left[\frac{q}{1-\alpha} - \frac{k^2\alpha}{1-\alpha} - \left[\frac{1}{2}\frac{\nabla^2\alpha}{1-\alpha} + \frac{(\nabla\alpha)^2}{4(1-\alpha)^2}\right]\right] + \frac{\alpha V_c}{1-\alpha}, \quad (2)$$

where $\alpha(r)$ and $q(r)$ arise from p and s-wave pion-nucleon interaction, respectively. Both are complex and energy dependent and obey the following equations:

$$q(r) = -4\pi P_1(b_0\rho(r) - e_\pi b_1\Delta\rho(r)) + \Delta q(r) \quad (3)$$

$$\alpha(r) = \frac{\alpha_1(r)}{1 + \frac{1}{3}\zeta\alpha_1(r)} + \alpha_2(r), \quad (4)$$

where

$$\alpha_1(r) = 4\pi\frac{(c_0\rho(r) - e_\pi c_1\Delta\rho(r))}{P_1} \quad (5)$$

$$\alpha_2(r) = 4\pi\frac{(C_0\rho_{np}(r) - e_\pi C_1\rho(r)\Delta\rho(r))}{P_2} \quad (6)$$

and

$$\rho(r) = \rho_n(r) + \rho_p(r) \quad (7)$$

$$\Delta\rho(r) = \rho_n(r) - \rho_p(r) \quad (8)$$

$$\rho_{np} = 4\rho_n(r)\rho_p(r) \quad (9)$$

Here e_π takes $+/-$ sign relative to the $+/-$ charge state of pions and $\rho_p(r)$ and $\rho_n(r)$ are proton and neutron density distributions in target nucleus, respectively. P_1 and P_2 are kinematic constants which depend on pion energy, where $P_1 = 1 + \epsilon$, $P_2 = 1 + \frac{\epsilon}{2}$, and $\varepsilon = \frac{\omega}{Mc^2}$, where M is the mass of a nucleon. Here we ignore the second order s-wave contributions and we take $\zeta = 1$. The V_c^2 term arises from minimal coupling and we do not include it in our calculation.

3 Complex Phase Shift Analysis of Pion-Wave Function

The scattering phase shifts around the energy range of (3,3) resonance are considered to be complex numbers. The imaginary part of the complex phase shifts of partial waves represent the amount of their contribution in elastic processes. These complex phase shifts are included in attenuation coefficients or partial wave scattering amplitudes and they control the behavior of the scattering cross-section. The scattering amplitude is of the form

$$f(\theta) = \frac{1}{k}\sum_0^\infty (2l+1)\exp(i\delta_l)\sin((\delta_l)P_l(\cos\theta). \quad (10)$$

We know that only p and s-waves dominate pion-nucleon interaction [11]. Assuming for the moment that the partial waves associated with these dominations

are the only one, then the elastic scattering amplitude of pions are estimated as follows:

$$f_{\pi N} = \frac{3}{k}[\eta_{++}\mathbf{k}.\mathbf{k}^{'}\hat{T}_{\frac{3}{2}} + \eta_{-+}\mathbf{k}.\mathbf{k}^{'}\hat{T}_{\frac{1}{2}}]\hat{J}_{\frac{3}{2}} + [\eta_{+-}\mathbf{k}.\mathbf{k}^{'}\hat{T}_{\frac{3}{2}} + \\ + \eta_{--}\mathbf{k}.\mathbf{k}^{'}\hat{T}_{\frac{1}{2}}]\hat{J}_{\frac{1}{2}} + \frac{1}{k}[[\eta_{+-}\mathbf{k}.\mathbf{k}^{'}\hat{T}_{\frac{3}{2}} + \eta_{--}\mathbf{k}.\mathbf{k}^{'}\hat{T}_{\frac{1}{2}}]\hat{J}_{\frac{1}{2}}, \quad (11)$$

where

$$\eta_l = \exp(i\delta_l)\sin(\delta_l). \quad (12)$$

The KOP in momentum or coordinate space is calculated from the transition matrix $< \mathbf{k}'\|t\|\mathbf{k} >$ of pion-nucleon scattering, which has a close relation with $f_{\pi N}(\theta)$. $\hat{J}_{\frac{1}{2}}$, $\hat{J}_{\frac{3}{2}}$, $\hat{T}_{\frac{1}{2}}$, and $\hat{T}_{\frac{3}{2}}$ in Eq. (11) represent the total angular momentum and isospin of pion-nucleon system. The plus and minus sign indices of η are equal to $\frac{3}{2}$ and $\frac{1}{2}$ for both spin and isospin values. The first sign is for isospin and the second sign represents spin values. Giving a sufficient attention to reference [11], it is obvious that P_{++}, S_{+-}, and S_{--} resonances are the dominant ones. Therefore, only the coefficient of these resonances should be kept. Now we choose the following form for the inelasticity coefficient, ξ_l:

$$\xi_l = \exp(-2\Im\delta_l) \quad (13)$$

from which we have

$$\eta_l = \exp(\imath\delta')\xi_l^{\frac{1}{2}}\sin\Big(\delta' - \frac{i\ln\xi_l}{2}\Big). \quad (14)$$

Here δ' represents the real part of δ_l. Substitution of Eq. (13) in (10) the scattering amplitudes of pions from nucleons for s and p-waves acquire additional coefficients. Continuing the calculations we find that the KOP also contains these coefficients and final expression for Eq. (1) is now given by

$$V_{op}(r) = \frac{(\hbar c)^2}{2\omega}(a_0 q(r) + a_1\nabla.\rho(r)\nabla), \quad (15)$$

where

$$a_0 = \frac{1}{k}\Big[\exp(i\delta'_{+-})\xi_{+-}^{\frac{1}{2}}\sin\Big(\delta'_{+-} - \frac{i\ln\xi_{+-}}{2}\Big) + \\ + \exp(i\delta'_{--})\xi_{--}^{\frac{1}{2}}\sin\Big(\delta'_{--} - \frac{i\ln\xi_{--}}{2}\Big)\Big] \quad (16)$$

$$a_1 = \frac{3}{k}\Big[\exp(i\delta'_{++})\xi_{++}^{\frac{1}{2}}\sin\Big(\delta'_{++} - \frac{i\ln\xi_{++}}{2}\Big) + \exp(i\delta'_{+-})\xi_{+-}^{\frac{1}{2}} \\ \times\sin\Big(\delta'_{+-} - \frac{i\ln\xi_{+-}}{2}\Big) + \exp(i\delta'_{--})\xi_{--}^{\frac{1}{2}}\sin\Big(\delta'_{--} - \frac{i\ln\xi_{--}}{2}\Big)\Big]. \quad (17)$$

The real parts of the phase shifts can be extracted from data [11]. Therefore, the KOP becomes as a parametric potential with respect to ξ. Data points are fitted with the theoretical expression of the differential cross-section for the elastic scattering of pions from a given nucleus in a given energy. Doing so an acceptable value for ξ is calculated at that energy. Repeating the fitting procedure for different energies one can calculate a fitting function for ξ as a function of dynamical variables. Here we have used the Born approximation to calculate the angular distribution, but instead of using Eq. (15) for KOP we have used its first form Eq. (1), with a distorted wave function for incident pions

$$\psi^d_{k'i} = N(r)\exp(i\mathbf{k}'.\mathbf{r}), \tag{18}$$

where

$$\mathbf{k}'_\mathbf{i} = (\alpha(\xi) + i\beta(\xi))\mathbf{k_i}. \tag{19}$$

Here α and β should have a smooth variation with energy and N is a function of energy, distance, and scattering angle. The following equation is proposed for it:

$$N = (A_1 r_1^B + iA_2 r_2^B)\sin(\theta_{sc}). \tag{20}$$

Now the amplitude for the elastic scattering of pions from a given nucleus is

$$f(\theta_{sc}) = -\Big(\frac{\mu}{2\pi\hbar^2}\Big)\int \exp(-i\mathbf{k_f}.\mathbf{r})U_L\psi^d_{\mathbf{k}'i}d^3r, \tag{21}$$

Where U_L is substituted from Eq. (2). To check the effect of the target density distribution on angular distributions we have illustrated our calculation for three model distributions named as two and three parameter Fermi distributions (2PF,3PF) and also Gaussian distribution (G). The 3PF form for proton (i=p) and neutron (i=n) to be used in Eqs. (7,8) is

$$\rho_i(r) = \rho_{0i}\frac{\Big(1+\dfrac{\omega_i r^2}{c_i^2}\Big)}{1+\exp\Big(\dfrac{r-c_i}{a_i}\Big)}. \tag{22}$$

The 2PF form is obtained from the above equation with $\omega_i = 0$. The G form used in $\pi - C$ scattering amplitude is

$$\rho(r) = \rho_0(1+\eta r^2)\exp\Big(-\frac{r^2}{a_\rho^2}\Big) \tag{23}$$

where

$$\rho_0 = \frac{4}{A(\sqrt{\pi}a_\rho)^3}, \quad \eta = \frac{(A-4)}{6a_\rho^2}. \tag{24}$$

Here $a_\rho = 1.68$ fm. The Fermi parameter values used in this paper are written in Table 1.

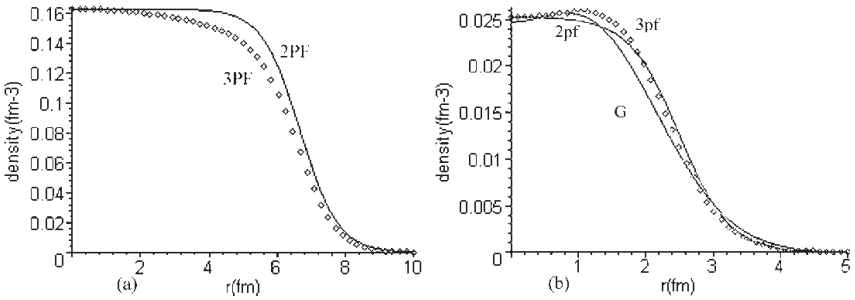

Figure 1. Density distribution of (a) – $^{208}_{82}$Pb, (b) – $^{12}_{6}$C according to 2PF, 3PF, and G forms.

4 Results and Discussions

We report our results for the elastic differential cross-sections for a heavy $^{208}_{82}$Pb target in which surface and volume effects are quite well separated and a light $^{12}_{6}$C target where the two effects overlap. Using Eqs. (21–23) the density distributions for these nuclei are displayed in Figures 1(a) and 1(b). The $< r^2 >^{\frac{1}{2}}$ values calculated from 2PF and 3PF forms for Pb are 5.545 fm and 5.437 fm. These values for carbon are 2.35 fm and 2.375 fm. The values of the potential parameters c_0, c_1, b_0 ,b_1, C_0, and C_1 are presented in Table 2. These parameters are energy dependent and their values are obtained by fitting the theoretical angular distribution to the experimental data values for different energy values. The potential curves for Pb are plotted in Figures 2(a), 2(b), and 2(c). They are constant within a radius 5.2–4.2 fm depending on energy, but display a sort of variation similar to density distribution at the surface region. The dependence of the potential on the gradients of density distributions are responsible for this surface structure. The real parts are mostly positive except for a very thin surface region. The repulsive real parts at each like points for 2PF distribution is stronger at higher energies, but this variation for 3PF form is quite unusual. This unusual behavior is much obvious for imaginary parts. The attractive real parts are sensitive to energy variation, becoming repulsive for higher energies. Three kinds of potential curves for carbon have nearly similar behaviors, but show an

Table 1. Parameters for Fermi forms of density distributions.

Nucleus	Model	c_p (fm)	ω_p	a_p (fm)	c_n (fm)	a_n (fm)	ω_n	Ref.
$^{208}_{82}$Pb	3PF	6.5800	-0.1760	0.5450	6.8	0.5450	-0.1760	[7]
	2PF	6.5800	0.0000	.5450	6.8	0.5450	0.000	[7]
$^{12}_{6}$C	3Pf	2.002	0.5400	0.3830	2.002	.383	0.5400	[12]
	2PF	2.5	0.0000	0.3700	2.5	0.3700	0.000	[13]

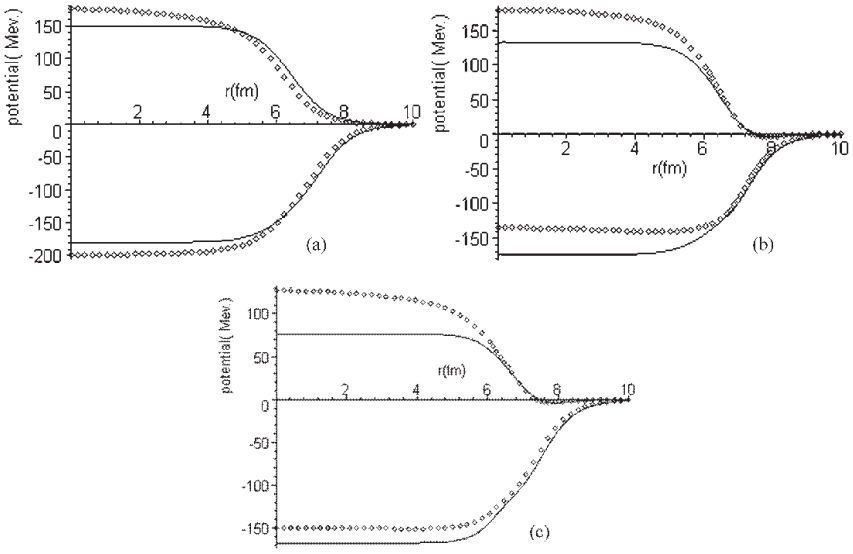

Figure 2. The real (repulsive upper curves) and imaginary(attractive lower curves) parts of equivalent local potential, U_L, for $\pi^- + {}^{208}_{82}$Pb at (a) – 162 MeV, (b) – 180 MeV, (c) – 291 MeV energies. The square shape curves and the continuous curves belong to 3PF and 2PF distributions respectively.

opposite trend of energy dependence both for real and imaginary parts in comparison with the heavy target Pb, Figures 3(a) and 3(b). Although the slope of the potentials for the 3PF is different from the 2PF curves, but they reach the same values at the thin surface region. There is no real attractive tail for

Table 2. Local potential parameter values calculated in this work with $\zeta = 1$. Note that in each column the left number is the real part and the right number is the imaginary part of the parameter.

Nucleus	T_π (MeV)	b_0 (fm)	b_1 (fm)	c_0 (fm^3)	c_1 (fm^3)	C_0 (fm^6)	C_1 (fm^6)
${}^{208}_{82}$Pb	162	0.179;	-0.126;	0.0296;	0.2764;	0.433;	2.227;
		-0.012	0.004	0.554	1.630	1.620	4.477
	180	-0.085;	-0.124;	0.146;	0.082;	3.058;	0.172;
		0.045	0.007	0.639	0.159	2.138	4.514
	291	-0.435;	-0.118;	-0.101;	-0.056;	0.728;	-0.599;
		0.135	0.020	0.651	0.121	0.469	1.183
${}^{12}_{6}$C	150	-6.079;	-0.012;	1.495;	0.276;	0.433;	2.227;
		5.041	0.005	0.554	0.276	2.120	4.477
	280	-4.716;	-0.136;	1.385;	0.256;	0.343;	1.227;
		4.250	0.015	0.534	0.377	2.226	4.452

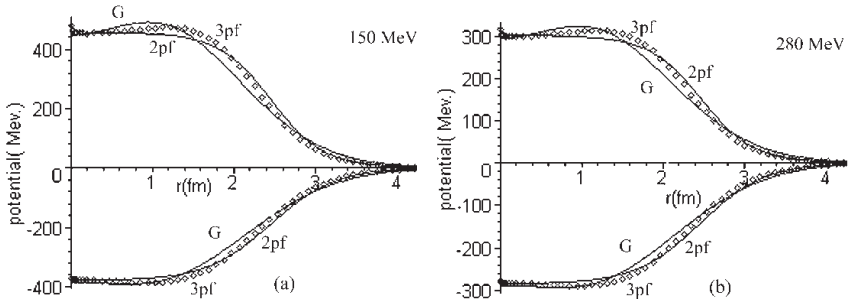

Figure 3. The real (repulsive curves) and imaginary (attractive curves) parts of equivalent local potential, U_L, for $\pi^- + {}^{12}_{6}\mathrm{C}$ at (a) – 150 MeV, (b) – 280 MeV.

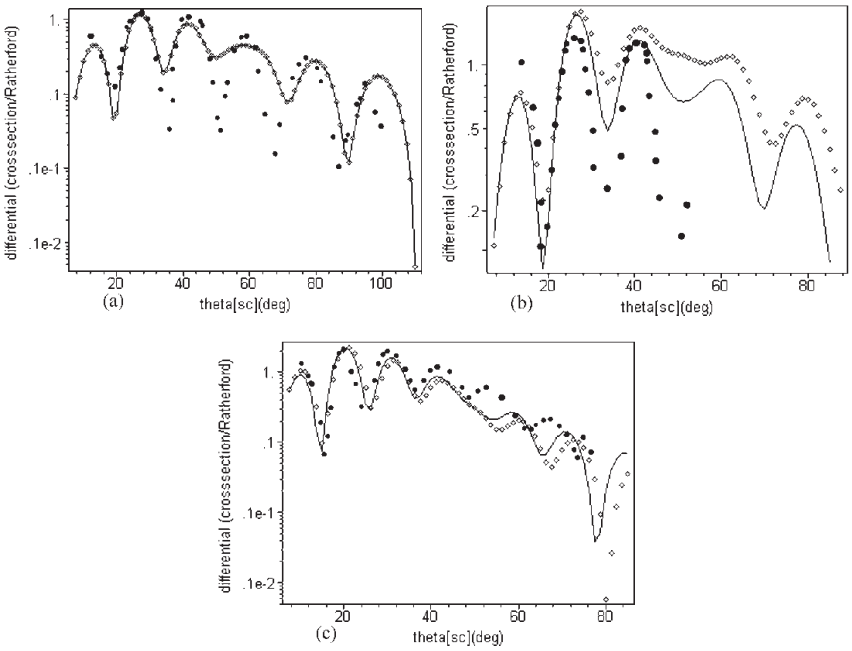

Figure 4. Elastic scattering differential cross-section of negative pion from $^{208}_{82}$Pb target using Eq. (21) at a – 162 MeV, b – 180 MeV, c – 291 MeV energies. Data points are from [14], [15], and [16] respectively. The square shape curves and the continuous curves belong to 3PF and 2PF distributions respectively.

the light carbon target. The differential elastic cross section has been calculated using Eq. (20) by using Simpson's numerical method of integration by dividing to 300 segments the distance of nuclear radius. Comparison of the differential cross-section of Eq. (21) relative to the respective Ratherford differential cross

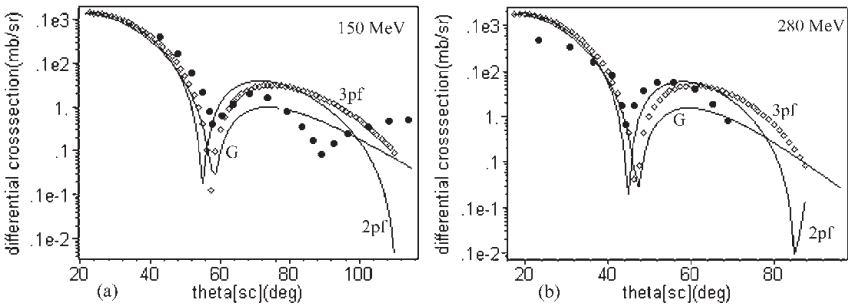

Figure 5. Elastic scattering differential cross-section of negative pion from $^{6}_{12}$C target using Eq. (21) at a – 150 MeV, b – 280 MeV. Data points are from [17].

section with corresponding data points at each energy is given in Figures 4(a), 4(b), and 4(c) for Pb and Figures 5(a) and 5(b) for carbon target. It is obvious that the theoretical and experimental results are almost the same in details. The consistency is better with increasing energy, and the 2PF results display a better agreement with data. The differences at large angles for lower energies might be explained by giving some theoretical considerations about the interaction parameters or rearranging a subtle experimental set ups for measuring the elastic scattering differential cross sections. In conclusion we suggest that to a good approximation, a local form of KOP along with choosing a suitable wave function for incident projectile can be used in Born approximation to have an acceptable estimate of angular distributions for elastic and in-elastic scattering of pions from nuclei.

Table 3. Wave function and kinematic parameter values calculated in this work.

Nucleus	T_π (MeV)	α	β	A_1	B_1	A_2	B_2	k (fm^{-1})	k_{eff} (fm^{-1})	P_1	P_2
$^{208}_{82}$Pb	162	1.35	-0.02	4	0.08	0.7	0.6	1.353	1.826	1.324	1.162
	180	1.33	-0.03	4.5	0.08	- 0.8	0.6	1.454	1.935	1.344	1.172
	291	1.2	-0.185	6.2	0.08	- 0.7	0.6	2.060	2.5014	1.463	1.231
$^{12}_{6}$C	150	1.470	0.06	4.5	0.08	-0.7	0.6	1.25	1.85	3.038	2.019
	280	1.15	0.006	8.8	0.08	-0.7	0.60	1.93	2.229	3.916	2.458

References

[1] C.M.Chen, D.J. Ernst and Mikkel B. Johanson (1993) *Phys. Rev. C* **48** 541.

[2] A.A. Ebrahim and R.J. Peterson (1996) *Phys. Rev. C* **54** 2499.

[3] I.J. Abu-Raddad (2002) *Phys. Rev. C* **66** 064601.

[4] A.A. Ebrahim and S.A.E. Khallaf (2005) *ACTA PHYSICA POLONICA B* **36** 2071.

[5] A. Engel *et al.* (1993) *arXiv: nucl-th/9307008* **1**.

[6] L.S. Kisslinger (1955) *Phys. Rev.* **98** 761.
[7] M.B. Johnson and G.R. Satchler (1996) *Ann. Phys.* **248** 134.
[8] R. Safari (2003) *Int. J. Comput. and Numeric. analysis. and Appl.* **4** No. 1, 71.
[9] R. Safari (2005) *Ind. J. Phys.* **79** 89.
[10] M. Krell and T.E.O. Ericson (1969) *Nucl. Phys. B* **11** 521.
[11] R.A. Arndt *et al.* (1995) *Phys. Rev. C* **52** 2120.
[12] R. Alvarez del Castillo and N.B. de Takacsy (1991) *Phys. Rev. C* **43** 1389.
[13] M. Preedom *et al.* (1981) *Phys. Rev. C* **23** 1134.
[14] C. Olmer *et al.* (1980) *Phys. Rev. C* **21** 254.
[15] G.R. Satchler (1980) *Nucl. Phys. A* **21** 254.
[16] D.F. Geesamann *et al.* (1981) *Phys. Rev. C* **23** 2635.
[17] M.M. Sternheim *et al.* (1971) *Phys. Rev. Lett.* **25** 1500.